Key Interactions for Clathrin Coat Stability

Till Böcking,[1,4,*] François Aguet,[1] Iris Rapoport,[1,3] Manuel Banzhaf,[1,3] Anan Yu,[1,3,5] Jean Christophe Zeeh,[1,3] and Tom Kirchhausen[1,2,3,*]
[1]Department of Cell Biology
[2]Department of Pediatrics
Harvard Medical School, Boston, MA 02115, USA
[3]Program in Cellular and Molecular Medicine at Boston Children's Hospital, Boston, MA 02115, USA
[4]Centre for Vascular Research, University of New South Wales, Sydney NSW 2052 Australia
[5]Present address: Department of Molecular Biosciences, Rice Institute for Biomedical Research, Northwestern University, Evanston, IL 60208, USA
*Correspondence: till.boecking@unsw.edu.au (T.B.), kirchhausen@crystal.harvard.edu (T.K.)
http://dx.doi.org/10.1016/j.str.2014.04.002

SUMMARY

Clathrin-coated vesicles are major carriers of vesicular traffic in eukaryotic cells. This endocytic pathway relies on cycles of clathrin coat assembly and Hsc70-mediated disassembly. Here we identify histidine residues as major determinants of lattice assembly and stability. They are located at the invariant interface between the proximal and distal segments of clathrin heavy chains, in triskelions centered on two adjacent vertices of the coated-vesicle lattice. Mutation of these histidine residues to glutamine alters the pH dependence of coat stability. We then describe single-particle fluorescence imaging experiments in which we follow the effect of these histidine mutations on susceptibility to Hsc70-dependent uncoating. Coats destabilized by these mutations require fewer Hsc70 molecules to initiate disassembly, as predicted by a model in which Hsc70 traps conformational distortions during the auxilin- and Hsc70:ATP-mediated uncoating reaction.

INTRODUCTION

In eukaryotic cells, clathrin-coated vesicles mediate the internalization of cargo molecules such as nutrients, hormones, and lipoproteins. Clathrin assembles on the intracellular surface of the plasma membrane into closed lattices that drive membrane invagination (Brodsky et al., 2001; Edeling et al., 2006; Kirchhausen, 2000). After budding from the plasma membrane, the coated vesicle must rapidly shed its clathrin coat to allow fusion of the naked vesicle with its endosomal targets and recycling of coat components. This "uncoating" process is catalyzed by heat shock cognate protein 70 (Hsc70) (Schlossman et al., 1984), a molecular chaperone that is recruited to the coated vesicle by its cochaperone auxilin (Ungewickell et al., 1995). The timing of the uncoating reaction is determined by the association of auxilin with the coated vesicle just after scission from the membrane (Guan et al., 2010; Massol et al., 2006). Hsc70 functions as a simple ATP-driven molecular clamp that goes through cycles of substrate binding and release (Hartl and Hayer-Hartl, 2009).

In the ATP-loaded state, its substrate-binding domain is in an open conformation and binds to clathrin with fast on-rate and low affinity. ATP hydrolysis, triggered by interaction with the J-domain of auxilin and with its substrate, is coupled to a conformational change in the substrate-binding domain, resulting in a closed conformation and tight clathrin binding. Nucleotide exchange resets the cycle and leads to reopening of Hsc70 and substrate release. This process is catalyzed by nucleotide exchange factors such as Hsp110, which facilitates Hsc70-driven clathrin uncoating by promoting the dissociation of the Hsc70/ADP-clathrin complex (Morgan et al., 2013; Schuermann et al., 2008).

Our knowledge of the interactions involved in clathrin coat stability and disassembly is based largely on reconstitution of these processes in vitro. The basic assembly unit of the coat is the clathrin triskelion, a pinwheel-shaped molecule consisting of three ~190 kDa heavy-chain "legs" radiating from a trimeric hub and each associated with an ~30 kDa light chain (Figure 1). Purified clathrin triskelions self-assemble at slightly acidic pH into "cages" ranging in diameter from ~50 to 120 nm (Kirchhausen and Harrison, 1981; Pearse and Crowther, 1987). Clathrin adaptor proteins facilitate self-assembly (Keen, 1990), and the resulting structures, termed "coats," exhibit a narrower size distribution than do empty cages assembled without adaptor proteins (Pearse and Crowther, 1987). The structure of the hexagonal D6 barrel coat (Figure 1), assembled from clathrin and a fraction containing the heterotetrameric adaptor protein AP-2, has been obtained by electron cryomicroscopy (cryoEM) (Fotin et al., 2004b; Musacchio et al., 1999; Smith et al., 1998; Vigers et al., 1986). The "hub" of a triskelion (clathrin residues 1074–1675) is centered at each vertex of the coat. Each edge in the outer shell of the coat consists of two proximal legs from neighboring triskelions (Figure 1A), each with a distal leg from another triskelion running just below it. The extended radial contact between the parallel proximal and distal leg (Figure 1B) is the most extensive interface in the lattice and is invariant among coat structures with and without bound chaperones, suggesting that it determines the stability of the coat (Fotin et al., 2004b; Xing et al., 2010). The specific residues involved in stabilizing the clathrin coat have not yet been identified. The stability of the clathrin lattice is strongly pH dependent. At pH 6.0, clathrin cages and coats are very stable and even resist Hsc70-driven uncoating (Braell et al., 1984; Schmid and Rothman, 1985; Xing et al., 2010); at pH 7.5, the clathrin lattice spontaneously
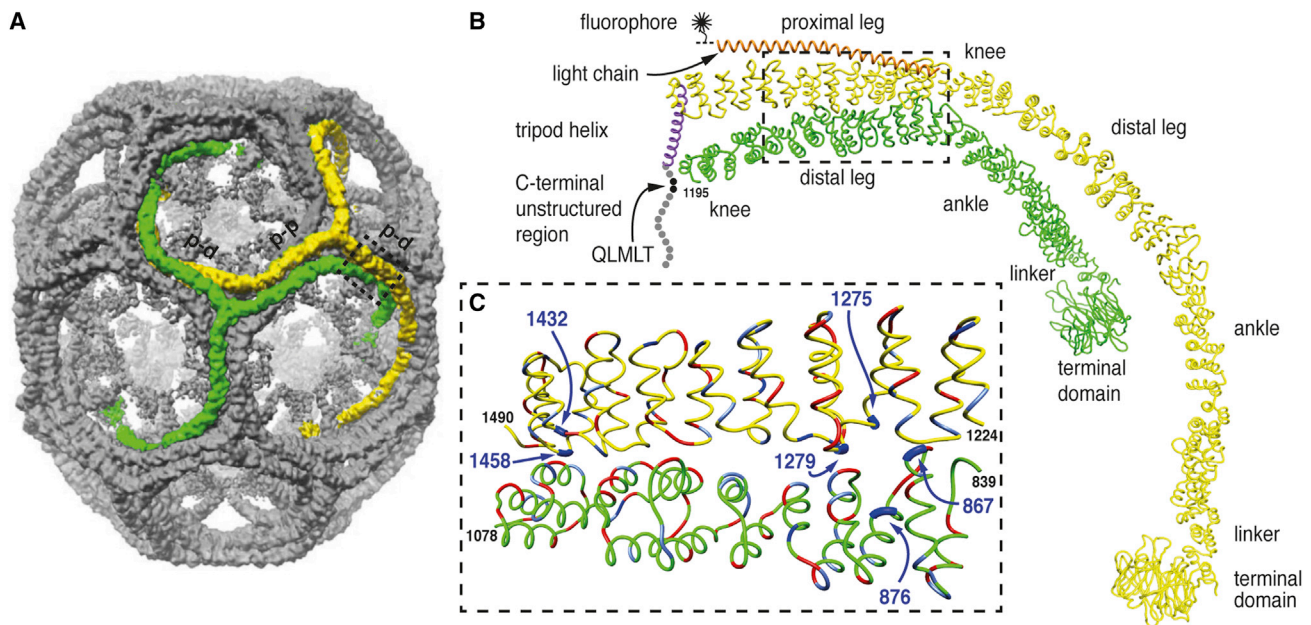
Figure 1. Location of Histidine Residues at the Contacts between Proximal and Distal Segments of Neighboring Triskelions

(A) Image reconstruction of a clathrin/AP-2 coat in the D6 barrel form (Fotin et al., 2004b). The contacts between parallel proximal and distal segments of the triskelions highlighted in green and yellow are indicated (p-d). The antiparallel proximal segments of the triskelions highlighted in green and yellow are indicated (p-p).

(B) α-carbon traces of single legs from neighboring triskelions (yellow and green) showing the invariant contact between parallel proximal and distal heavy-chain segments viewed from the side. The heavy-chain molecule shown in green comprises residues 1 to 1195 (includes part of the knee, distal leg, ankle, linker, and terminal domain). The yellow heavy chain is associated with the central helix of its bound light chain (orange) and the α helix of its trimerization domain, forming part of the C-terminal tripod of the triskelion (purple). The disordered region of the heavy chain (residues 1630–1675) is indicated by the spheres with the binding site for Hsc70 (QLMLT motif) shown in black. The central helical segment of clathrin light chain is shown in orange. For imaging, the light chain was labeled with a fluorophore at a single cysteine residue C-terminal to the helical segment.

(C) Close-up view of the interface between the proximal segment of the yellow heavy chain and the distal segment of the green heavy chain (indicated by the dashed box in A and B) viewed from the side. The histidine residues mutated in this study are shown in dark blue and indicated by the arrows. Negatively charged residues are shown in red and positively charged residues are shown in light blue.

depolymerizes (Pearse and Crowther, 1987). This pH dependence implicates the involvement of histidine residues, which have a pKa between 6.3 and 6.9.

Insight into the mechanism of Hsc70-driven clathrin coat disassembly comes from structural and biochemical studies of clathrin coats assembled in vitro. Up to three auxilin molecules bind beneath each vertex, where each auxilin associates with a terminal domain of a clathrin heavy chain and also makes contact with the ankle segments of two other triskelions (Fotin et al., 2004a). Auxilin positions Hsc70 on the inside of the coat, close to the inward-projecting C-terminal tripod formed by an extended helix from each heavy chain. In this location, Hsc70 can bind to a QLMLT consensus motif in the C-terminal unstructured region of clathrin heavy chain required for the uncoating reaction (Rapoport et al., 2008). A cryoEM reconstruction of an uncoating intermediate trapped at low pH shows that Hsc70 binds on the inner surface of the intact coat with a stoichiometry of approximately one molecule per vertex (Xing et al., 2010). Hsc70 binding leads to a distortion of the lattice (Xing et al., 2010). Using fluorescence microscopy, we have followed the uncoating reaction in real time (Böcking et al., 2011). In conjunction with the lattice distortion observed in the cryoEM structure (Xing et al., 2010), we proposed a model in which Hsc70 mole-

cules capture multiple destabilizing fluctuations of clathrin molecules for long enough to reinforce each other and lead to coat disassembly.

In the work described here, we have identified histidine residues at the interface of proximal and distal segments of clathrin heavy chains in a coat and show that mutating sets of these residues to glutamine destabilizes the coat. We have systematically altered the stability of the clathrin coat by exploiting its well-known pH sensitivity (Barouch et al., 1997; Braell et al., 1984; Schmid and Rothman, 1985) or by mutating the identified histidine residues to determine the effect of coat stability on the kinetics of the Hsc70-driven uncoating reaction. Using fluorescence microscopy and kinetic modeling, we show that coats destabilized by mutation of certain histidine residues require fewer Hsc70 molecules to initiate disassembly.

RESULTS

Role of Histidine Residues in Coat Stability

We identified six candidate histidine residues from the cryoEM structure of the clathrin coat (Fotin et al., 2004a) that might participate in electrostatic interactions and/or hydrogen bonds in the clathrin lattice. Residues H867 and H876 in the distal leg
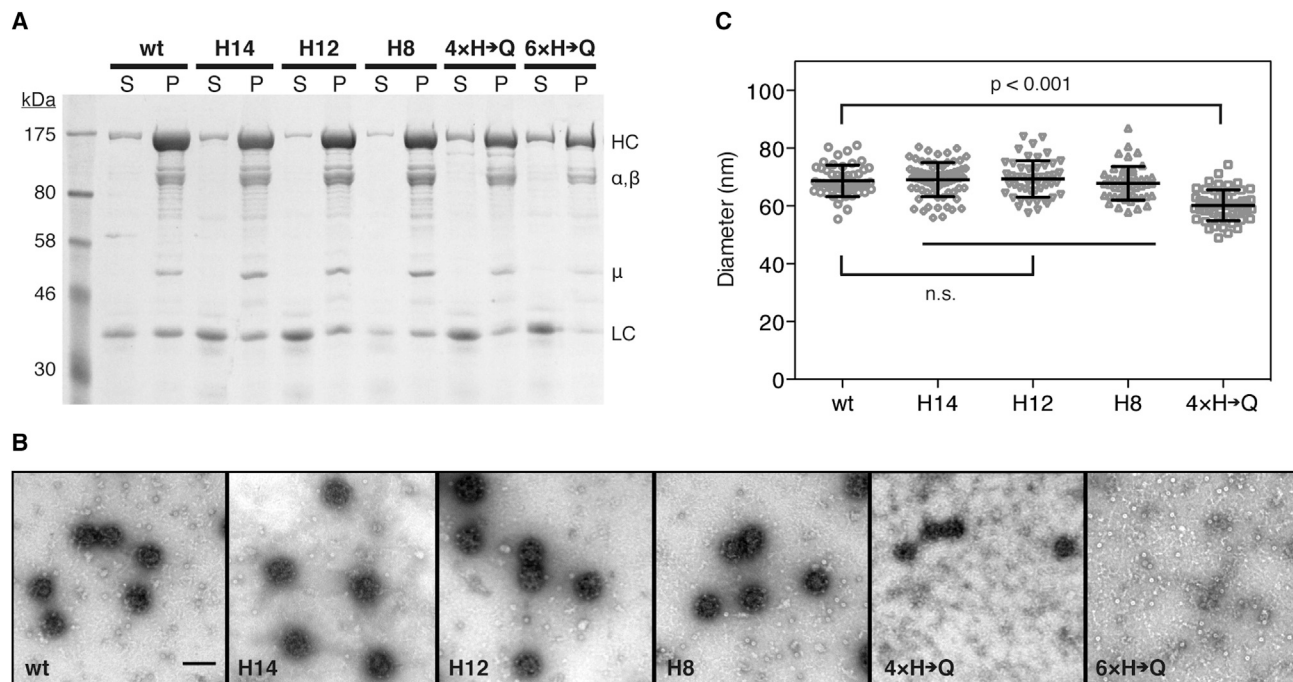
Figure 2. Clathrin Coat Assembly Using Wild-Type and Histidine Clathrin Mutants

(A) SDS-PAGE and Coomassie blue analysis of the high-speed centrifugation supernatant (S) and pellet (P) fractions of clathrin/AP-2 coats. α,β and μ-chain of AP-2; HC, clathrin heavy chain; LC, clathrin light chain.

(B) Electron micrographs of fields of negatively stained (1.2% uranyl acetate) clathrin/AP-2 coats assembled with wild-type clathrin heavy chain or histidine mutants. The scale bar represents 100 nm.

(C) Diameters of clathrin coats assembled with wild-type clathrin heavy chain or histidine mutants determined from the electron microscopic images. $n \geq 50$ coats were measured for each coat preparation; values are mean ± SD.

segment and residues H1275, H1279, H1432, and H1458 in the proximal leg segment are at the proximal-distal interface (see Figure 1 for details). Using the crystal structure of the heavy-chain residues 1210 to 1516 (Ybe et al., 1999), we further confirmed that the imidazole rings of the four candidate histidine residues in the proximal segment are oriented toward the interface with the distal segment. To test whether these residues are involved in stabilizing the coat, we generated three histidine to glutamine double mutants of rat clathrin heavy chain (H867Q/H876Q, H1275Q/H1279Q, and H1432Q/H1458Q, designated H8, H12, and H14, respectively). In addition, we generated a quadruple mutant by combining the double mutants H12 and H14 (designated 4 × H→Q) and a sextuple mutant combining all three double mutants (designated 6 × H→Q). Mutant clathrin heavy chains were expressed in insect cells and purified as triskelions. We then added recombinant clathrin light chain LCa1 to the purified heavy chain to reconstitute triskelions containing three heavy and three light chains.

We verified that both wild-type and mutant clathrin triskelions assemble into coats by in vitro association with an adaptor fraction highly enriched in the heterotetrameric clathrin adaptor AP-2; we refer to these coats as clathrin/AP-2 coats. SDS-PAGE analysis of the high-speed pellets collected after coat formation at pH 6.5 revealed that wild-type and mutant triskelions formed assemblies that cosedimented with AP-2 (Figure 2A). Clathrin light chain bound at similar or only slightly reduced levels (~70%–95%) to mutant clathrin coats compared with wild-type

clathrin coats, as estimated by densitometry of Coomassie-stained gels of several coat preparations. The yield of coats for the three double mutants H8, H12, and H14 was comparable with that of wild-type clathrin coats. Negative-stain electron micrographs of the resuspended pellets showed that these mutants formed coats with an appearance and diameter (~68–69 nm) indistinguishable from the D6 barrel coats formed by wild-type clathrin (Figures 2B and 2C) (Fotin et al., 2004b; Smith et al., 1998; Xing et al., 2010). The 4 × H→Q mutants assembled into homogeneous structures with an average diameter of ~60 nm, significantly smaller than wild-type coats (Figures 2B and 2C), and we therefore did not include these coats in further studies. Resuspended pellets of structures formed with clathrin triskelions containing all six histidine-to-glutamine mutations contained very few assembled structures; electron micrographs showed mainly free triskelions (Figure 2B). We conclude that the assemblies formed at high concentrations of 6 × H→Q clathrin and AP-2 (see Figure 1) dissociated rapidly upon resuspension of the high speed pellet at pH 6.5.

We devised a simple fluorescence microscopy assay to compare the stability of wild-type and mutant clathrin coats by measuring the loss of fluorescent triskelions from coats exposed to buffer solutions of increasing pH (Figure 3A). Spontaneous, uncatalyzed disassembly of in vitro clathrin structures occurs after dilution below a critical threshold (Crowther and Pearse, 1981; Kirchhausen and Harrison, 1981). We predicted that coats assembled with clathrin-lacking residues involved in stabilizing
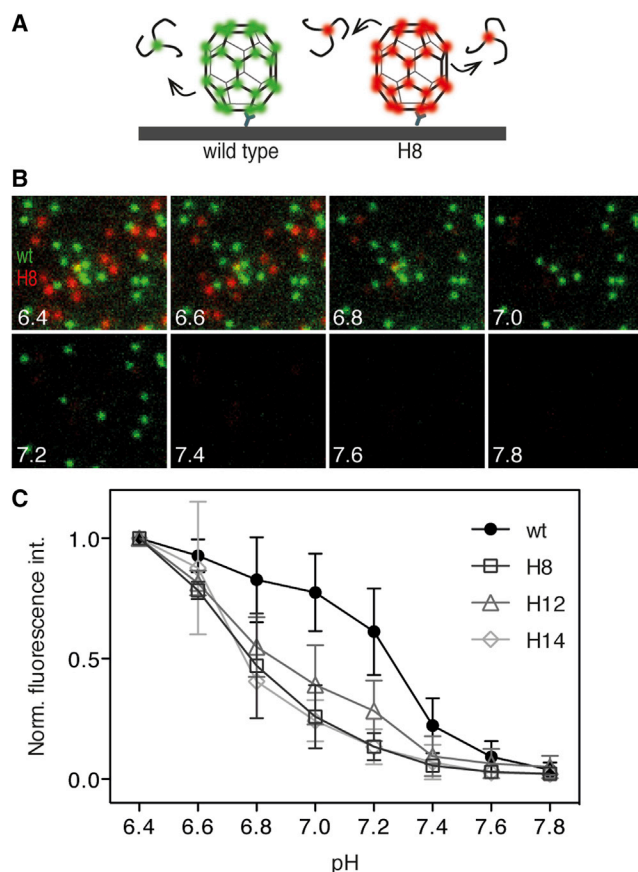
Figure 3. Clathrin Coats Assembled with Clathrin Heavy Chain Histidine Double Mutants Are Less Stable Than Wild-Type Coats at Higher pH

(A) Schematic representation of the fluorescence microscopy assay to measure coat stability. Clathrin/AP-2 coats assembled from fluorescent clathrin trimers were captured with an antibody directed against LCa1 onto a chemically modified coverslip and imaged using TIRF microscopy before and after exposure to buffer solutions of increasing pH.

(B) Representative images of clathrin/AP-2 coats assembled with wild-type clathrin labeled with LCa-AF488 and mutant H8 labeled with LCa-DL649 after exposure to buffer solutions in the pH range from pH 6.4 to pH 7.8.

(C) pH stability curves for clathrin/AP-2 coats assembly with wild-type clathrin or the histidine double mutant H14, H12, or H8; mean ± SD.
See also Figure S1.

the lattice would fall apart more readily with increasing pH than do wild-type coats. Wild-type coats labeled with Alexa Fluor 488 (Molecular Probes) and histidine double-mutant coats labeled with DyLight 649 (Pierce) were captured onto the same coverslip for observation by total internal reflection microscopy. Using microfluidic delivery, the coats were then exposed successively to buffer solutions of increasing pH and imaged 1 min after each solution exchange to determine the fluorescence intensity remaining for each type of coat.

A representative series of images comparing wild-type and H8 mutant coats in the range from pH 6.4 to pH 7.8 is shown in Figure 3B. From the images, it was immediately apparent that the mutant coats (red) disappeared at a lower pH threshold than wild-type coats. Individual coat signals within each population decreased to varying degrees at each pH step (Figure S1 avail-

able online), as expected for coats with variable contents of AP-2. The mean signal intensity relative to the signal at pH 6.4 for wild-type and mutant coats after each pH step is shown in Figure 3C. Wild-type coats dissociated to a limited extent up to pH 7.2, with minor decreases in the coat intensity after each step. At pH 7.4, most of the wild-type coat signal was lost rapidly; the signal reached background levels at pH 7.6. For coats assembled with histidine double mutants H8, H12, and H14, the fluorescence signal had fallen to about half its initial value at pH 6.4 when the pH reached pH 6.8 (Figure 3C). At pH 7.0, the mutant coats had essentially disappeared, while the wild-type coats were still largely intact. We conclude that histidine residues located at the interface between proximal and distal leg segments contribute to stabilizing contacts in the clathrin lattice.

Uncoating Reaction with Destabilized H14 Clathrin/AP-2 Coats

Our model for Hsc70-driven uncoating predicts that to dissociate coats destabilized by mutation would require fewer Hsc70 molecules than needed to dissociate wild-type coats. We used our single-particle fluorescence microscopy uncoating assay (Böcking et al., 2011) to measure chaperone binding and coat disassembly for individual coats (Figure 4). Fluorescent clathrin/AP-2 coats were captured onto a modified glass coverslip and immediately incubated with auxilin(547–910). Auxilin binding stabilized the clathrin coat (Ahle and Ungewickell, 1990; Scheele et al., 2001) and slowed the spontaneous dissociation of the H14 lattices; the auxilin(547–910)-loaded H14 coats remained intact at pH 6.8 (Figure 4E) in the absence of Hsc70-ATP. We then initiated the uncoating reaction by injecting a solution containing auxilin(547–910), Hsc70, and ATP into the flow channel while measuring the fluorescence intensities of the clathrin- and Hsc70-associated signals by time-lapse total internal reflection fluorescence (TIRF) microscopy with alternating fluorescence excitation. Wild-type and H14 mutant coats appeared in the fluorescence image as bright, diffraction-limited spots (Figure 4B, top row) which persisted after the addition of Hsc70-ATP for varying periods of time before disappearing rapidly as a result of coat disassembly (Figure 4B, bottom row, and Figure 4C). The onset of signal decay varied among individual coats in the population but occurred on average earlier for H14 mutant than wild-type coats.

Clathrin and Hsc70 fluorescence intensity traces extracted from the time-lapse images for each coat in the field of view exhibited typical uncoating kinetics (Böcking et al., 2011) for the wild-type coats (Figure 4D, wt). During an accumulation phase, the clathrin signal remained constant while the Hsc70 signal increased steadily. The clathrin- and Hsc70-associated signals started abruptly to decline to background at about the time at which the Hsc70 signal had reached its maximum. A small signal remained at the location of the coat in each channel, corresponding to the clathrin bound to the antibody on the coverslip surface and associated Hsc70 molecules. The H14 intensity traces (Figure 4D, H14) showed the same basic uncoating behavior characterized by an accumulation and a disassembly phase but with on average shorter accumulation times, as expected for the destabilized H14 clathrin lattice.

We used our kinetic model for the Hsc70-driven uncoating reaction (Figure 5A) (Böcking et al., 2011) to calculate the number
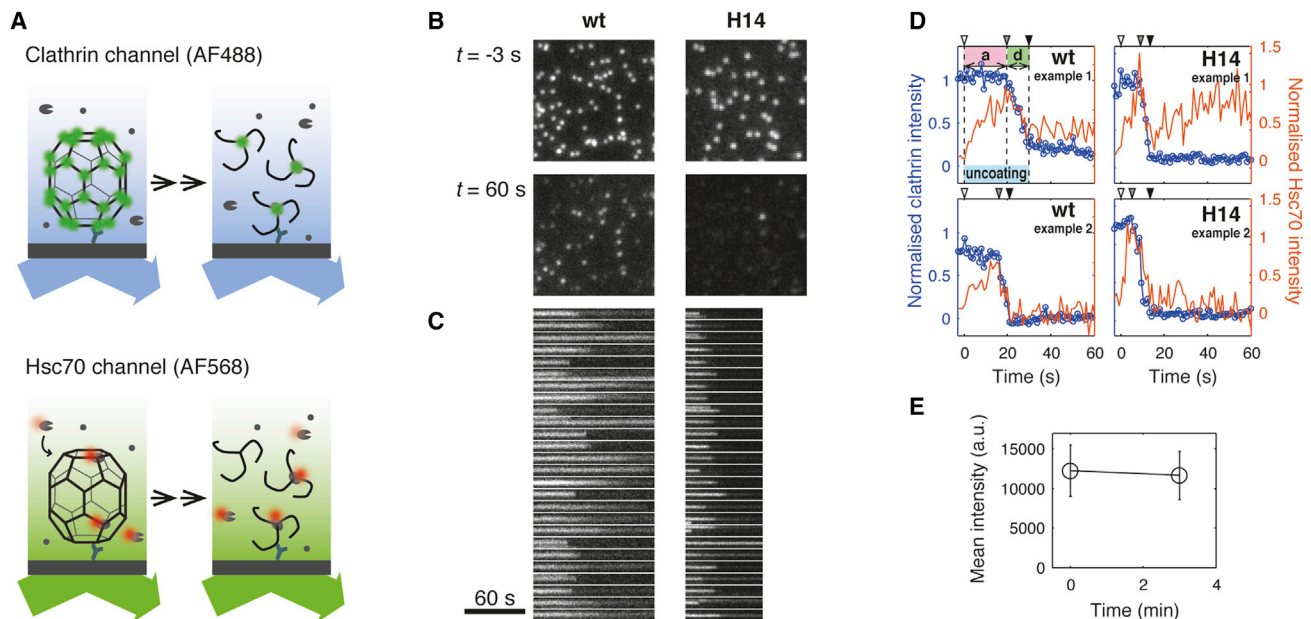
Figure 4. Single-Particle Uncoating Assay of Wild-Type and H14 Mutant Coats

(A) Schematic representation of the single-particle uncoating assay.

(B) Frames of the uncoating time series (120 × 120 pixel region for wild-type coats and 60 × 60 pixel region with 2 × 2 binning for H14 coats) showing the diffraction-limited signals from fluorescent coats loaded with auxilin(547–910) before (top) and 60 s after (bottom) the addition of 1.0 μM Hsc70-ATP at pH 6.8.

(C) Kymographs of the clathrin signal originating from coats contained in the images shown in (B).

(D) Representative uncoating traces for clathrin/AP-2 coats assembled with wild-type or H14 clathrin showing binding of Hsc70 to the coats during the accumulation phase (a) followed by rapid coat disassembly (d). The arrowheads indicate the arrival of Hsc70-ATP (t = 0, open arrowhead) and the start (gray arrowhead) and end (black arrowhead) of the disassembly phase. The intensity trace of the clathrin signal is shown in blue, and the intensity trace of the Hsc70 signal is shown in orange.

(E) Fluorescence intensities (mean ± SD) of H14 clathrin/AP-2 coats before (top, N = 581 coats) and after (bottom, N = 611 coats) exposure to buffer solution (pH 6.8) containing 1.3 μM auxilin(547–910) for 3 min.

of Hsc70 molecules required to initiate disassembly for wild-type and H14 coats at pH 6.8 (Figure 5B, top and bottom panels, respectively). We model binding of Hsc70 to the intact coat with a maximum occupancy of one molecule per vertex (Xing et al., 2010) and a single rate constant for association (k_1^+) and dissociation (k_1^-) at any of the N = 36 vertices. The values of these rate constants (k_1^+ = 0.07 μM^{-1} s^{-1} and k_1^- = 0.027 s^{-1}) were determined previously from Hsc70 binding curves measured at a range of Hsc70 concentrations (Böcking et al., 2011). We further assume that upon reaching a certain threshold level, N_t, of Hsc70 loading, the coat transitions to disassembly with a single rate-limiting step of rate constant k_2^+. We fixed this rate constant at an average value of k_2^+ = 0.13 s^{-1} (see Experimental Procedures for details), similar to that determined independently (Böcking et al., 2011). A numerical fit of the rate equations to the accumulation time distributions (Figure 5B, pink) obtained from several hundred single-particle uncoating traces yielded estimates of the threshold level N_t as the only free model parameter. This threshold level represents the average number of Hsc70 molecules that need to be associated with the coat to trigger the transition to the disassembly phase. The total number of Hsc70 molecules required for complete coat disassembly is larger because binding to the coat continues throughout the transition and disassembly steps.

The accumulation times of H14 coats (~10 s) were on average considerably shorter than those of wild-type coats (~30 s).

Kinetic modeling showed that a mutant coat had bound less than half of the amount of Hsc70 when it commits to uncoating (N_t = 10) than does a wild-type coat (N_t = 23). Disassembly (Figure 5B, green) proceeds as a single exponential decay, with a single rate-limiting step of rate constant k_3^+. Mutant coat disassembly was only marginally faster than wild-type coat disassembly. The complete kinetic model for accumulation and disassembly (Figure 5A) gave an excellent fit of the distributions of times for the entire uncoating reaction (Figure 5B, blue) when using the values for N_t and k_3^+ determined as described above.

At pH 6.6, the uncoating kinetics for wild-type and mutant coats were indistinguishable (Figure S2) in contrast to the pronounced differences described above for pH 6.8. This observation is not surprising because the intrinsic stabilities of the wild-type and mutant coats are comparable at pH 6.6, whereas mutant coats are considerably less stable than wild-type coats at pH 6.8 (Figure 3C). These analyses suggest that the Hsc70-driven uncoating of H14 coats proceeds with the same basic mechanism as for wild-type coats but that the destabilized H14 coats require a lower threshold of Hsc70 binding to initiate disassembly.

Dependence of the Uncoating Reaction on pH

To investigate further the effect of coat stability on the uncoating reaction, we varied the strength of the interactions between
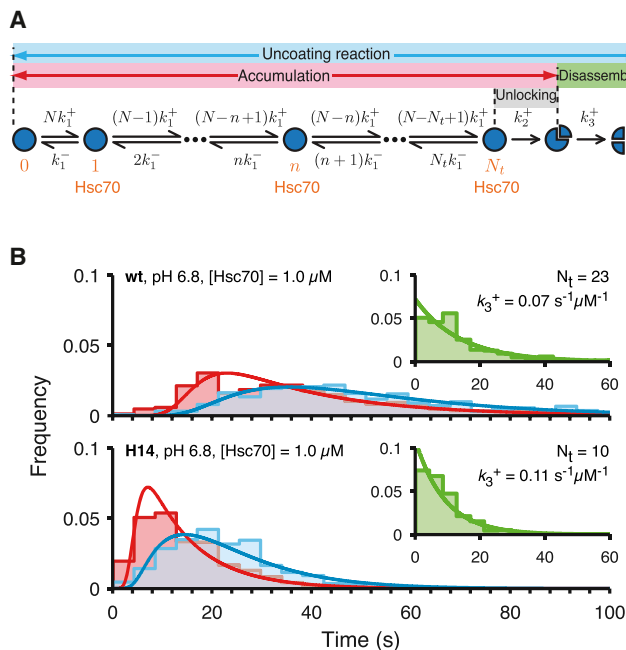
A

B

Figure 5. Kinetic Model of the Uncoating Reaction

(A) Scheme of the kinetic model.

(B) Distributions of Hsc70 accumulation times (red), disassembly times (green), and the full uncoating reaction times (blue) overlaid with fits of the kinetic model. The uncoating reaction was carried out with wild-type or H14 mutant coats at pH 6.8 in the presence of 1.0 μM Hsc70.

See also Figure S2.

triskelions in the wild-type clathrin lattice by varying the pH in the narrow range between pH 6.4 and pH 7.2 and following the uncoating reaction by single-particle fluorescence imaging. Although disassembly is not synchronized between individual coats at a given pH, the average persistence time of the coat signal depends strongly on pH, as evident from the snapshots at 60 s after injection of auxilin(547–910) and Hsc70-ATP (Figure 6A) and the corresponding kymographs (Figure 6B) and single-particle traces (Figure 6C). The coats are very stable at pH 6.4. As a consequence, most coat signals (85%) remain high during the time of the imaging assay (200 s), while the disappearance of the remainder occurs only after a long delay of typically 30 to 50 s after injection of the uncoating reagents. As the pH is increased, the coat signals persist for increasingly shorter periods of time. At pH 7.2, the vast majority of coat signals (>90%) have decayed to background within 14 s after injection of the uncoating reagents. Concomitant with the acceleration of the uncoating reaction, there is a pronounced increase in the uncoating efficiency from pH 6.4 (15%) to pH 6.6 (88%); close to 100% uncoat at pH $\geq$ 7.0 (Figure 6D), just as do clathrin cages in a bulk uncoating assay (Schmid and Rothman, 1985). The single-particle traces (Figure 6C) for the majority of coats at pH $\geq$ 6.6 showed the characteristic Hsc70 accumulation phase followed by rapid clathrin disassembly. In contrast, most clathrin signals observed at pH 6.4 remained constant or decreased only slowly despite efficient Hsc70 binding to a steady-state level (Figure 6C). Thus, clathrin coats are effectively locked at pH 6.4, in agreement with previous observations at low

pH (Braell et al., 1984; Xing et al., 2010), but undergo normal Hsc70-driven uncoating at pH $\geq$ 6.6.

To determine whether the differences in uncoating kinetics could be explained by an effect of pH on the rate of Hsc70 binding, we averaged the Hsc70 traces of coats that remain intact (Figure 6E). The mean Hsc70 binding curves determined at each pH were the same (Figure 6E), indicating that pH did not have a measurable effect on the recruitment of Hsc70 between pH 6.6 and pH 7.2. Binding followed first-order kinetics, and the observed rate constant for Hsc70 association determined from a fit of the curves ($k_{obs} \approx 0.14$ s^{-1} for [Hsc70] = 1.3 μM; Figure 6E) was consistent with the previously determined Hsc70 association rate constant, across a range of Hsc70 concentrations (Böcking et al., 2011). The pH independence of the initial binding phase could also be seen from the mean intensity traces of coats that proceeded to disassembly (Figure 6F). These traces did not reach a plateau, and the mean intensity decreased as soon as the signals of disassembling coats started to disappear. As expected, this turning point occurred earlier at higher pH values. Nevertheless, the initial parts of the mean curves were superimposable. We conclude that the pronounced effects of pH on the outcome of the uncoating reaction is due primarily to coat stability and not driven by changes in Hsc70 recruitment.

Analysis of the accumulation time distributions measured at different pH (Figure 7, pink) with the kinetic model shown in Figure 5A yielded estimates of the threshold level N_t as a function of pH (see Experimental Procedures for details of the model parameters). The pronounced shift of the accumulation time distributions to shorter times with increasing pH was reflected by a sharp drop in N_t between pH 6.8 (N_t = 22) and pH 7.2 (N_t = 4) (Figures 7 and 8A). We determined the fluorescence intensity ratio of the Hsc70 and clathrin signals from all single-particle uncoating traces at the onset of coat disassembly to obtain a measure that is proportional to the number of bound Hsc70 molecules. The average Hsc70:clathrin intensity ratio (Figure 8B) confirmed the sharp drop with increasing pH in the amount of bound Hsc70 at the time of disassembly. Thus, the specific binding of a few Hsc70 molecules to the relatively unstable coat at pH 7.2 is sufficient to trigger the release of the first triskelion(s). Analysis of the kinetic data also showed that the disassembly rate constant increased as a function of pH (Figure 8C), demonstrating that the Hsc70-dependent uncoating proceeds more rapidly when coats are destabilized by higher pH.

DISCUSSION

We have prepared histidine-to-glutamine mutants of clathrin heavy chain that at pH close to neutral assemble in vitro into clathrin/AP-2 coats more unstable than those assembled from wild-type clathrin. Using single-particle fluorescence imaging to examine the effect of pH on coat stability and the effect of coat stability on the kinetics of the Hsc70/ATP and auxilin-dependent uncoating reaction, we draw the following principal conclusions: (1) The pH dependence of coat stability derives at least in part from titration of histidine residues at the proximal-distal contact. (2) The number of structural perturbations required to remove triskelions from the coat and the rate of uncoating depend on the overall stability of the clathrin lattice: the less stable the coat, the smaller the number of Hsc70
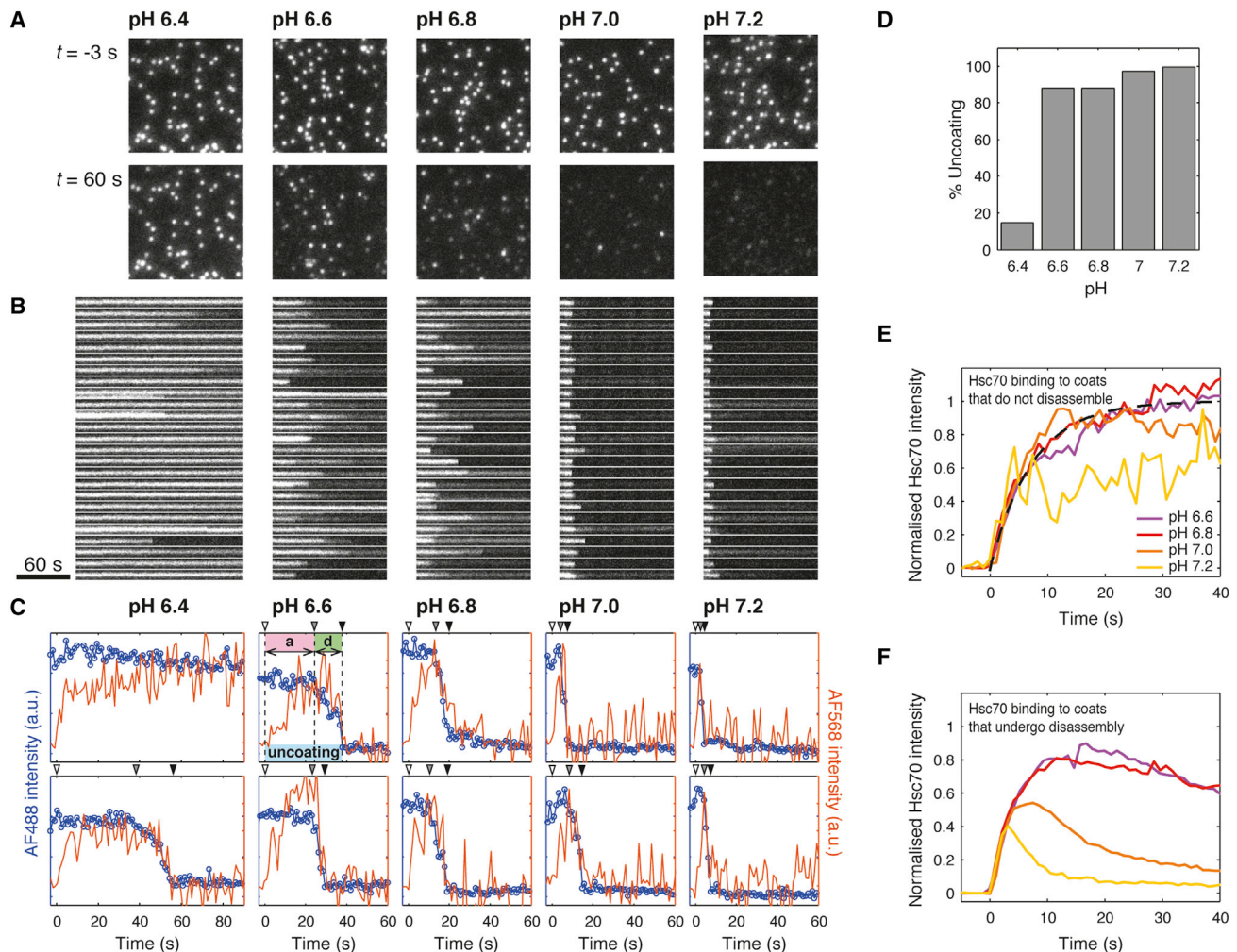
Figure 6. Single-Particle Uncoating Assay at Various pH Values

(A) Frames of the uncoating time series (120 × 120 pixel region from a 512 × 512 pixel image) showing the diffraction-limited signals from AF-488 coats loaded with auxilin(547–910) before (top) and 60 s after (bottom) the addition of 1.0 μM Hsc70-ATP at pH values between 6.4 and 7.2.

(B) Kymographs of the clathrin signal originating from coats contained in the images shown in (A).

(C) Representative uncoating traces for clathrin/AP-2 coats showing binding of Hsc70 to the coats during the accumulation phase (a) followed by rapid coat disassembly (d). The arrowheads indicate the arrival of Hsc70-ATP (t = 0, open arrowhead) and the start (gray arrowhead) and end (black arrowhead) of the disassembly phase. The intensity trace of the clathrin signal is shown in blue, and the intensity trace of the Hsc70 signal is shown in orange.

(D) Uncoating efficiency of wild-type clathrin/AP-2 coats between pH 6.4 and pH 7.2.

(E and F) Hsc70 binding to the coats during the accumulation phase is not pH dependent. The colored traces correspond to the average binding curves of Hsc70-ATP to coats in uncoating assays conducted between pH 6.6 and pH 7.2 for coats that remain intact (F; average of N = 86, 93, 17, and 3 traces for pH 6.6, 6.8, 7.0, and 7.2, respectively) or those that undergo uncoating (F; average of N = 624, 683, 617, and 846 traces for pH 6.6, 6.8, 7.0, and 7.2, respectively). The dotted line represents a fitted association curve.

molecules that must bind before uncoating can begin and the faster the disassembly. (3) Auxilin binding stabilizes coats. (4) Binding of Hsc70 to a vertex is independent of coat stability, and the effects of pH on the kinetics of uncoating do not result from differences in Hsc70 recruitment.

Molecular Interactions and Coat Stability

Guided by the structural model of the clathrin/AP-2 coat determined by cryoEM, we identified six histidine residues of clathrin heavy chain located at the contact between the proximal and distal legs of neighboring triskelions in the coat and mutated

them in pairs to glutamine to obtain three double mutants. All three double mutants assembled into stable D6 barrel coats at pH 6.5 with comparable yield to wild-type clathrin, but mutant coats dissociated more readily than wild-type clathrin coats at pH ≥ 6.8. Assemblies formed with clathrin containing all six mutations were unstable when resuspended even at pH 6.5, a condition under which wild-type coats are extremely stable. These observations are consistent with the structural model prediction that the proximal-distal contact is the main determinant of coat stability. This prediction is based on the strong structural conservation of the proximal/distal interface observed in the
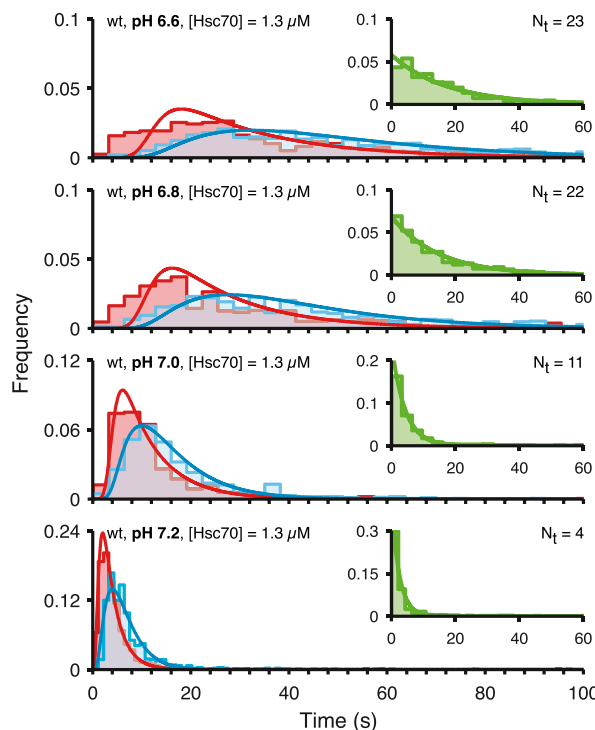
Figure 7. pH Dependence of the Uncoating Kinetics
Distributions of Hsc70 accumulation times (red), disassembly times (green), and the times of the entire uncoating reaction (blue) overlaid with fits of the kinetic model. The uncoating reaction was carried out with wild-type coats at various pH values in the range between pH 6.6 and 7.2 in the presence of 1.3 μM Hsc70.

histidine residues would be insufficient to stabilize assemblies consisting of just a few triskelions. Thus, assembling structures would exhibit low stability at the very early stages of assembly and need to be stabilized by other factors to survive. The latter has been observed in growing clathrin-coated pits at the plasma membrane. Clathrin-coated pits that are not stabilized by cargo binding to adaptor proteins, especially AP-2 (Höning et al., 2005; Jackson et al., 2010), do not proceed to a complete clathrin-coated vesicle but disassemble rapidly, leading to the observation of so-called abortive pits (Aguet et al., 2013; Ehrlich et al., 2004; Loerke et al., 2009).

Mechanism of Clathrin Uncoating
Each triskelion is linked to its nearest neighbors by six proximal-distal contacts (Figure 1). Release of a triskelion or a group of triskelions may occur when a sufficient number of proximal-distal contacts break simultaneously. The probability of release increases when proximal-distal contacts are weakened by strain induced by Hsc70 binding.

Auxilin, originally isolated as a clathrin assembly protein, stabilizes clathrin coats in vitro (Ahle and Ungewickell, 1990). It binds to one of three equivalent binding sites underneath the vertex, where it makes contact with two ankle segments and a terminal domain of three different triskelions (Fotin et al., 2004a; Scheele et al., 2001). At high concentrations of auxilin, when all binding sites are occupied, it stabilizes a conformational change at the junction between the ankle and distal segment of a triskelion leg (Fotin et al., 2004a). As expected, auxilin bound at high concentrations slowed the spontaneous release of triskelions from the coat, consistent with the view that the interactions with three different triskelions effectively "crosslink" the coat. Thus, the free energy of auxilin binding more than offsets the energy cost of distorting the ankle crossing. During the uncoating reaction, Hsc70-ATP is recruited by the J-domain of auxilin to a location just underneath the ankle crossing, where it can bind to the QLMLT motif in the unstructured C-terminal tail of clathrin heavy chain beneath the triskelion hub (Rapoport et al., 2008). Interaction with the clathrin substrate and the J-domain leads to ATP hydrolysis and closure of the substrate-binding groove, leading to tight association with clathrin and weakening of the contact with the J-domain of auxilin (Hartl and Hayer-Hartl, 2009). Tight binding of Hsc70 enhances the displacement of the ankle of one or more triskelions forming the ankle crossing. This displacement leads to a strain that could propagate to destabilize the proximal-distal contact (Xing et al., 2010). At this point, auxilin may dissociate, further destabilizing the lattice. Additional binding of Hsc70 to other vertices leads to weakening of a sufficient number of proximal-distal contacts so that the cooperative release of triskelions (the uncoating reaction) can now ensue.

We observed that the uncoating rate increased with increasing pH values. Mutation of histidine to glutamine residues at the proximal-distal contact has the same effect. Faster uncoating correlates with a lower threshold in the number of bound Hsc70 required for the cooperative release of triskelions. The coincident breaking of proximal-distal contacts may represent a rate-limiting step after association of a sufficient number of Hsc70 molecules. The point of disassembly is reached before Hsc70 binding has reached stoichiometric levels of binding,
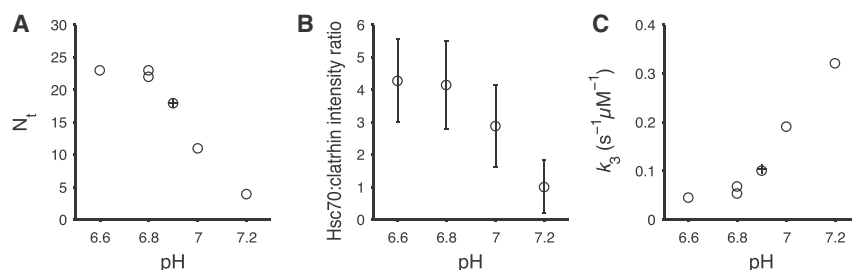
cryoEM structures of coats with two different symmetries and in native and auxilin-bound D6 barrels (Fotin et al., 2004b; Xing et al., 2010).

We speculate that the pH dependence of coat stability derives at least in part from titration of the interfacial histidine residues tested here: as the pH is increased from 6.4 to 7.2, fewer histidines protonate, decreasing the density of stabilizing interactions. Removal of some of these interactions by mutation appears to have the same destabilizing effect, which becomes measurable in our assay at pH $\geq$ 6.8. The uncoating reaction of coats assembled in vitro is rapid at pH values that would be expected for the cytoplasm (pH 7.0–7.4) and kinetic modeling of the uncoating data at pH 7.2 shows that binding of a few Hsc70 molecules is sufficient to initiate disassembly. This observation suggests that the clathrin lattice by itself is poised for disassembly at the pH values encountered in the cytosol, and rapid uncoating can be initiated with few perturbations.

At cytosolic pH, only a (small) proportion of histidine residues are protonated, which leads to the following picture of coat stability: the coat as a whole is sufficiently stabilized by a network of electrostatic interactions that are distributed randomly all over the coat. (Note that a D6 barrel coat with 36 triskelions contains 324 of the double-histidine sites examined in this study.) The distribution of stabilizing contacts may be dynamic, allowing structural fluctuations to occur while maintaining overall lattice integrity. In contrast, the interactions mediated by protonated

Figure 8. Destabilized Clathrin Lattices Require Less Hsc70 to Initiate Disassembly and Fall Apart Faster

(A) Number of Hsc70 molecules per coat (N_t) required to commit the reaction to disassembly as a function of pH determined by kinetic modeling; Open circles represent data from Figures 5 and 7 and control experiments; plus sign represents average N_t determined previously across a range of Hsc70 concentrations (Böcking et al., 2011).

(B) Average ratio of the Hsc70:clathrin fluorescence intensities (mean ± SD) determined for each trace at the time point just prior to coat disassembly (average of N = 624, 683, 617, and 846 traces for pH 6.6, 6.8, 7.0, and 7.2, respectively).

(C) Rate constant k_3^+ describing the disassembly phase as a function of pH determined by kinetic modeling. Open circles represent data from Figures 5 and 7 and control experiments; plus sign represents average k_3^+ determined previously across a range of Hsc70 concentrations (Böcking et al., 2011).

whereby the average threshold for disassembly depends on the overall stability of the coat, which is determined by the strength of the proximal-distal contact. Thus, fewer perturbations induced by Hsc70 binding are required for disassembly when the proximal-distal contacts are intrinsically weakened by elevated pH or by the clathrin mutations used in this study.

On the basis of recent biochemical studies (Young et al., 2013), it has been proposed that the clathrin light chains might be involved in the uncoating reaction, because the efficiency with which auxilin can mediate the uncoating reaction decreases in their absence. Our observations show that the increased uncoating with the mutant coats do not depend on light chains, because they bind equally well to wild-type and histidine mutant triskelions.

To conclude, our results confirm two predictions. The first concerns the source of lattice stability in the clathrin coat. We identified a set of histidine residues, at the invariant interface between the proximal and distal legs of two triskelions, that contribute to the assembly and stability of the clathrin lattice. The second prediction concerns the mechanism of chaperone-mediated uncoating. A key component of the proposed uncoating mechanism is trapping by Hsc70 of destabilizing fluctuations in the clathrin lattice. Weakening interactions in the coat should decrease the number of trapped distortions required to disassemble the lattice. The effect of the histidine mutations on uncoating susceptibility is consistent with this prediction.

EXPERIMENTAL PROCEDURES

Proteins

Fluorescent clathrin was reconstituted from recombinant rat clathrin heavy chain trimers and recombinant rat clathrin light chain (LCa1 D203E/C218S) labeled with maleimide-derivatized fluorophores (Alexa Fluor 488, Alexa Fluor 568, or DyLight 649) as previously described (Böcking et al., 2011). Bovine Hsc70 was expressed, purified, and labeled at an added C-terminal cysteine residue using Alexa Fluor 568 C₅ maleimide (Böcking et al., 2011). Bovine auxilin(547–910) containing the J-domain and clathrin-binding sites was expressed and purified as previously described (Rapoport et al., 2008).

Coat Formation

Recombinant clathrin triskelions were mixed with an adaptor fraction isolated from calf brain and highly enriched in AP-2 (Rapoport et al., 2008) at a ratio of 3:1 (w/w). The mixture was dialyzed against coat formation solution (50 mM MES [pH 6.5], 100 mM NaCl, 2 mM EDTA, 0.5 mM dithiothreitol) at 4°C for 14 hr with one solution exchange. After removal of aggregates by low-speed

centrifugation (TLA 100.4 rotor [Beckman Coulter], 12,000 rpm, 10 min, 4°C), the coats were harvested by ultracentrifugation (TLA 100.4 rotor, 65,000 rpm, 14–16 min, 4°C) and resuspended in coat formation solution at a concentration of ~1 mg/ml.

Electron Microscopy

Diluted solutions of the coats were applied to carbon-coated electron microscopy grids immediately after cleaning by glow discharge and blotted with filter paper. The samples were stained with a freshly prepared solution of 1.2% (w/v) uranyl acetate, blotted, and air dried. Electron micrographs were obtained using a Tecnai G² Spirit BioTWIN at a primary magnification of 30,000×. Coat diameters were measured using ImageJ (NIH), and data sets were compared using one-way ANOVA and Tukey's multiple comparison test using Prism (GraphPad Software).

Surface Chemistry and Flow Cell Preparation

Glass coverslips were cleaned by sonication in ethanol (30 min) and 1 M NaOH (30 min), followed by rinsing with ultrapure water, drying, and treatment in a glow-discharge unit. The glass surface was covered with a solution of the copolymer PLL(20)-g[3.4]-PEG(2)/PEG(3.4)-biotin (20%) (Susos) in PBS (1 mg/ml) for 30 min and rinsed with ultrapure water. The surface was then covered with a solution of streptavidin (0.2 mg/ml in 20 mM Tris [pH 7.5], 2 mM EDTA, 50 mM NaCl, 0.03% NaN₃, 0.025% Tween 20, 0.2 mg/ml BSA), incubated for 30 min, and rinsed with ultrapure water. The microfluidic flow cell was assembled by clamping a polydimethylsiloxane device with microfluidic channels (80 μm high and 800 μm wide) onto the modified glass coverslip. A syringe pump was used to pull solutions through the microfluidic channels.

Capture of Clathrin Coats and TIRF Microscopy

The biotinylated antibody CVC.6 directed against clathrin LCa was immobilized on the surface of the coverslip modified with streptavidin. Fluorescent clathrin coats were flowed through the microfluidic channel and captured onto the surface of the coverslip via the antibody. A brief pulse (1–2 μl of ~0.1 mg/ml coats in coat formation solution) was sufficient to capture several hundred coats per field of view. Images were acquired sequentially for the different fluorophores using an inverted microscope (Zeiss 200M) with TIRF slider and Alpha Plan-Apo 100× objective (1.46 NA). Solid-state lasers (488, 561, and 640 nm) were used for excitation and an electron-multiplying charge-coupled device camera (QuantEM 512 SC; Photometrics) for detection of fluorescence emission.

Clathrin Coat Stability Assay

Wild-type and mutant clathrin coats each labeled with different fluorophores were captured onto the surface of the coverslip and exposed to buffer solutions (50 mM imidazole, 100 mM KCl, 2 mM MgCl₂) adjusted to increasing pH values (pH 6.4–7.8 in steps of 0.2 pH units). Solutions were exchanged in the microfluidic channels by flowing 30 μl buffer solution at a flow rate of 30 μl/min. A single fluorescence image in each channel was recorded at the end of an incubation period (1 min) at each pH value to determine the loss

of fluorescence signal of wild-type and mutant clathrin coats. Under these imaging conditions photobleaching was negligible.

Single-Particle Uncoating Assay

Auxilin was bound to the coats immediately after their capture onto the coverslip by flowing a solution of 0.05 mg/ml (1.3 μM) auxilin(547–910) in uncoating solution (20 mM imidazole [pH 6.8], 100 mM KCl, 2 mM MgCl$_2$) through the microfluidic channel. To initiate the uncoating reaction, a mixture containing Hsc70-AF568 at various concentrations, 0.02 mg/ml (0.5 μM) auxilin(547–910), and 2 mM ATP in uncoating solution was injected into the microfluidic channel at a flow rate of 100 μl/min. Image acquisition was started just prior to injection of the uncoating reagents. Images were acquired with an exposure of 2 to 10 ms and a frequency of 1 to 2 frames per second. The antioxidant trolox (2 mM) and an oxygen-quenching system consisting of protocatechuic acid (2.5 mM) and protocatechuate-3,4-dioxygenase (0.25 U/ml) were used to minimize photobleaching (Aitken et al., 2008).

Image Analysis and Kinetic Modeling

Fluorescence images were analyzed using algorithms coded in MATLAB (The MathWorks). The fluorescence intensity traces for clathrin and Hsc70 were calculated by Gaussian fitting of the corresponding diffraction-limited signals in each channel. The beginning ($t = 0$) of the reaction was defined as the arrival time of the labeled Hsc70-ATP at the coverslip surface and determined from the appearance of fluorescence background in the Hsc70 channel. We then used an algorithm based on automated step fitting of each single-particle trace (Kerssemakers et al., 2006) to determine the time point at which the clathrin signal started to decay and the time point at which the clathrin signal had reached a stable level close to the background. Coats that undergo an uncoating reaction were defined as those traces exhibiting a phase of rapid signal disappearance. Kinetic modeling to determine the critical number of Hsc70 molecules (N_t) required to initiate disassembly was carried out as described previously (Böcking et al., 2011). We found little variation in the value of k_2^+ obtained by numerical fits of the rate equations to the accumulation time distributions for uncoating experiments conducted with wild-type coats at pH 6.8 ($k_2^+ = 0.13 \pm 0.05$ s^{-1}) and fixed k_2^+ at the average value for analysis of the data in Figure 5. Further, the value of k_2^+ was only weakly dependent on pH in the range between pH 6.6 and pH 7.0. Numerical fits of the accumulation time distributions with k_2^+ as a free model parameter yielded estimates of $k_2^+ = 0.1$, 0.13, and 0.16 s^{-1} for pH 6.6, 6.8, and 7.0, respectively. Fits with a fixed value of $k_2^+ = 0.13$ s^{-1} described these distributions equally well and yielded estimates for N_t of 24, 22, and 9 for pH 6.6, 6.8, and 7.0, respectively. A higher value of $k_2^+ = 0.38$ s^{-1} was required for the fit of the accumulation time distribution at pH 7.2. The uncoating kinetics and estimates for N_t determined for wild-type coats labeled with either Alexa Fluor 488 or DyLight649 were indistinguishable, showing that the type of fluorophore used for clathrin labeling did not affect the outcome of the single-particle uncoating assay.

SUPPLEMENTAL INFORMATION

Supplemental Information includes two figures and can be found with this article online at http://dx.doi.org/10.1016/j.str.2014.04.002.

AUTHOR CONTRIBUTIONS

T.B. and T.K. designed the experiments. F.A. and T.B. performed data analysis and modeling. A.Y. (clathrin mutants), I.R. (protein expression and purification, coat formations), J.C.Z. (pH stability assay), M.B. (electron microscopy, pH stability assay), T.B. (uncoating assay), and T.K. (electron microscopy) carried out the experiments. T.B. and T.K. wrote the manuscript. All authors discussed the results and commented on the manuscript.

REFERENCES

Aguet, F., Antonescu, C.N., Mettlen, M., Schmid, S.L., and Danuser, G. (2013). Advances in analysis of low signal-to-noise images link dynamin and AP2 to the functions of an endocytic checkpoint. Dev. Cell *26*, 279–291.

Ahle, S., and Ungewickell, E. (1990). Auxilin, a newly identified clathrin-associated protein in coated vesicles from bovine brain. J. Cell Biol. *111*, 19–29.

Aitken, C.E., Marshall, R.A., and Puglisi, J.D. (2008). An oxygen scavenging system for improvement of dye stability in single-molecule fluorescence experiments. Biophys. J. *94*, 1826–1835.

Barouch, W., Prasad, K., Greene, L., and Eisenberg, E. (1997). Auxilin-induced interaction of the molecular chaperone Hsc70 with clathrin baskets. Biochemistry *36*, 4303–4308.

Böcking, T., Aguet, F., Harrison, S.C., and Kirchhausen, T. (2011). Single-molecule analysis of a molecular disassemblase reveals the mechanism of Hsc70-driven clathrin uncoating. Nat. Struct. Mol. Biol. *18*, 295–301.

Braell, W.A., Schlossman, D.M., Schmid, S.L., and Rothman, J.E. (1984). Dissociation of clathrin coats coupled to the hydrolysis of ATP: role of an uncoating ATPase. J. Cell Biol. *99*, 734–741.

Brodsky, F.M., Chen, C.Y., Knuehl, C., Towler, M.C., and Wakeham, D.E. (2001). Biological basket weaving: formation and function of clathrin-coated vesicles. Annu. Rev. Cell Dev. Biol. *17*, 517–568.

Crowther, R.A., and Pearse, B.M. (1981). Assembly and packing of clathrin into coats. J. Cell Biol. *91*, 790–797.

Edeling, M.A., Smith, C., and Owen, D. (2006). Life of a clathrin coat: insights from clathrin and AP structures. Nat. Rev. Mol. Cell Biol. *7*, 32–44.

Ehrlich, M., Boll, W., Van Oijen, A., Hariharan, R., Chandran, K., Nibert, M.L., and Kirchhausen, T. (2004). Endocytosis by random initiation and stabilization of clathrin-coated pits. Cell *118*, 591–605.

Fotin, A., Cheng, Y., Grigorieff, N., Walz, T., Harrison, S.C., and Kirchhausen, T. (2004a). Structure of an auxilin-bound clathrin coat and its implications for the mechanism of uncoating. Nature *432*, 649–653.

Fotin, A., Cheng, Y., Sliz, P., Grigorieff, N., Harrison, S.C., Kirchhausen, T., and Walz, T. (2004b). Molecular model for a complete clathrin lattice from electron cryomicroscopy. Nature *432*, 573–579.

Guan, R., Dai, H., Harrison, S.C., and Kirchhausen, T. (2010). Structure of the PTEN-like region of auxilin, a detector of clathrin-coated vesicle budding. Structure *18*, 1191–1198.

Hartl, F.U., and Hayer-Hartl, M. (2009). Converging concepts of protein folding in vitro and in vivo. Nat. Struct. Mol. Biol. *16*, 574–581.

Höning, S., Ricotta, D., Krauss, M., Späte, K., Spolaore, B., Motley, A., Robinson, M., Robinson, C., Haucke, V., and Owen, D.J. (2005). Phosphatidylinositol-(4,5)-bisphosphate regulates sorting signal recognition by the clathrin-associated adaptor complex AP2. Mol. Cell *18*, 519–531.

Jackson, L.P., Kelly, B.T., McCoy, A.J., Gaffry, T., James, L.C., Collins, B.M., Höning, S., Evans, P.R., and Owen, D.J. (2010). A large-scale conformational change couples membrane recruitment to cargo binding in the AP2 clathrin adaptor complex. Cell *141*, 1220–1229.

Keen, J.H. (1990). Clathrin and associated assembly and disassembly proteins. Annu. Rev. Biochem. *59*, 415–438.

Kerssemakers, J.W.J., Munteanu, E.L., Laan, L., Noetzel, T.L., Janson, M.E., and Dogterom, M. (2006). Assembly dynamics of microtubules at molecular resolution. Nature *442*, 709–712.

Kirchhausen, T. (2000). Clathrin. Annu. Rev. Biochem. *69*, 699–727.

Kirchhausen, T., and Harrison, S.C. (1981). Protein organization in clathrin trimers. Cell *23*, 755–761.

Loerke, D., Mettlen, M., Yarar, D., Jaqaman, K., Jaqaman, H., Danuser, G., and Schmid, S.L. (2009). Cargo and dynamin regulate clathrin-coated pit maturation. PLoS Biol. *7*, e57.

Massol, R.H., Boll, W., Griffin, A.M., and Kirchhausen, T. (2006). A burst of auxilin recruitment determines the onset of clathrin-coated vesicle uncoating. Proc. Natl. Acad. Sci. U S A *103*, 10265–10270.

Morgan, J.R., Jiang, J., Oliphint, P.A., Jin, S., Gimenez, L.E., Busch, D.J., Foldes, A.E., Zhuo, Y., Sousa, R., and Lafer, E.M. (2013). A role for an Hsp70 nucleotide exchange factor in the regulation of synaptic vesicle endocytosis. J. Neurosci. *33*, 8009–8021.

Musacchio, A., Smith, C.J., Roseman, A.M., Harrison, S.C., Kirchhausen, T., and Pearse, B.M. (1999). Functional organization of clathrin in coats: combining electron cryomicroscopy and X-ray crystallography. Mol. Cell *3*, 761–770.

Pearse, B.M., and Crowther, R.A. (1987). Structure and assembly of coated vesicles. Annu. Rev. Biophys. Biophys. Chem. *16*, 49–68.

Rapoport, I., Boll, W., Yu, A., Böcking, T., and Kirchhausen, T. (2008). A motif in the clathrin heavy chain required for the Hsc70/auxilin uncoating reaction. Mol. Biol. Cell *19*, 405–413.

Scheele, U., Kalthoff, C., and Ungewickell, E. (2001). Multiple interactions of auxilin 1 with clathrin and the AP-2 adaptor complex. J. Biol. Chem. *276*, 36131–36138.

Schlossman, D.M., Schmid, S.L., Braell, W.A., and Rothman, J.E. (1984). An enzyme that removes clathrin coats: purification of an uncoating ATPase. J. Cell Biol. *99*, 723–733.

Schmid, S.L., and Rothman, J.E. (1985). Enzymatic dissociation of clathrin cages in a two-stage process. J. Biol. Chem. *260*, 10044–10049.

Schuermann, J.P., Jiang, J., Cuellar, J., Llorca, O., Wang, L., Gimenez, L.E., Jin, S., Taylor, A.B., Demeler, B., Morano, K.A., et al. (2008). Structure of the Hsp110:Hsc70 nucleotide exchange machine. Mol. Cell *31*, 232–243.

Smith, C.J., Grigorieff, N., and Pearse, B.M. (1998). Clathrin coats at 21 A resolution: a cellular assembly designed to recycle multiple membrane receptors. EMBO J. *17*, 4943–4953.

Ungewickell, E., Ungewickell, H., Holstein, S.E., Lindner, R., Prasad, K., Barouch, W., Martin, B., Greene, L.E., and Eisenberg, E. (1995). Role of auxilin in uncoating clathrin-coated vesicles. Nature *378*, 632–635.

Vigers, G.P., Crowther, R.A., and Pearse, B.M. (1986). Three-dimensional structure of clathrin cages in ice. EMBO J. *5*, 529–534.

Xing, Y., Böcking, T., Wolf, M., Grigorieff, N., Kirchhausen, T., and Harrison, S.C. (2010). Structure of clathrin coat with bound Hsc70 and auxilin: mechanism of Hsc70-facilitated disassembly. EMBO J. *29*, 655–665.

Ybe, J.A., Brodsky, F.M., Hofmann, K., Lin, K., Liu, S.H., Chen, L., Earnest, T.N., Fletterick, R.J., and Hwang, P.K. (1999). Clathrin self-assembly is mediated by a tandemly repeated superhelix. Nature *399*, 371–375.

Young, A., Stoilova-McPhie, S., Rothnie, A., Vallis, Y., Harvey-Smith, P., Ranson, N., Kent, H., Brodsky, F.M., Pearse, B.M.F., Roseman, A., and Smith, C.J. (2013). Hsc70-induced changes in clathrin-auxilin cage structure suggest a role for clathrin light chains in cage disassembly. Traffic *14*, 987–996.

Supplemental Information

Key Interactions for Clathrin Coat Stability

Till Böcking, François Aguet, Iris Rapoport, Manuel Banzhaf, Anan Yu, Jean Christophe Zeeh, and Tom Kirchhausen

Supplemental Figures
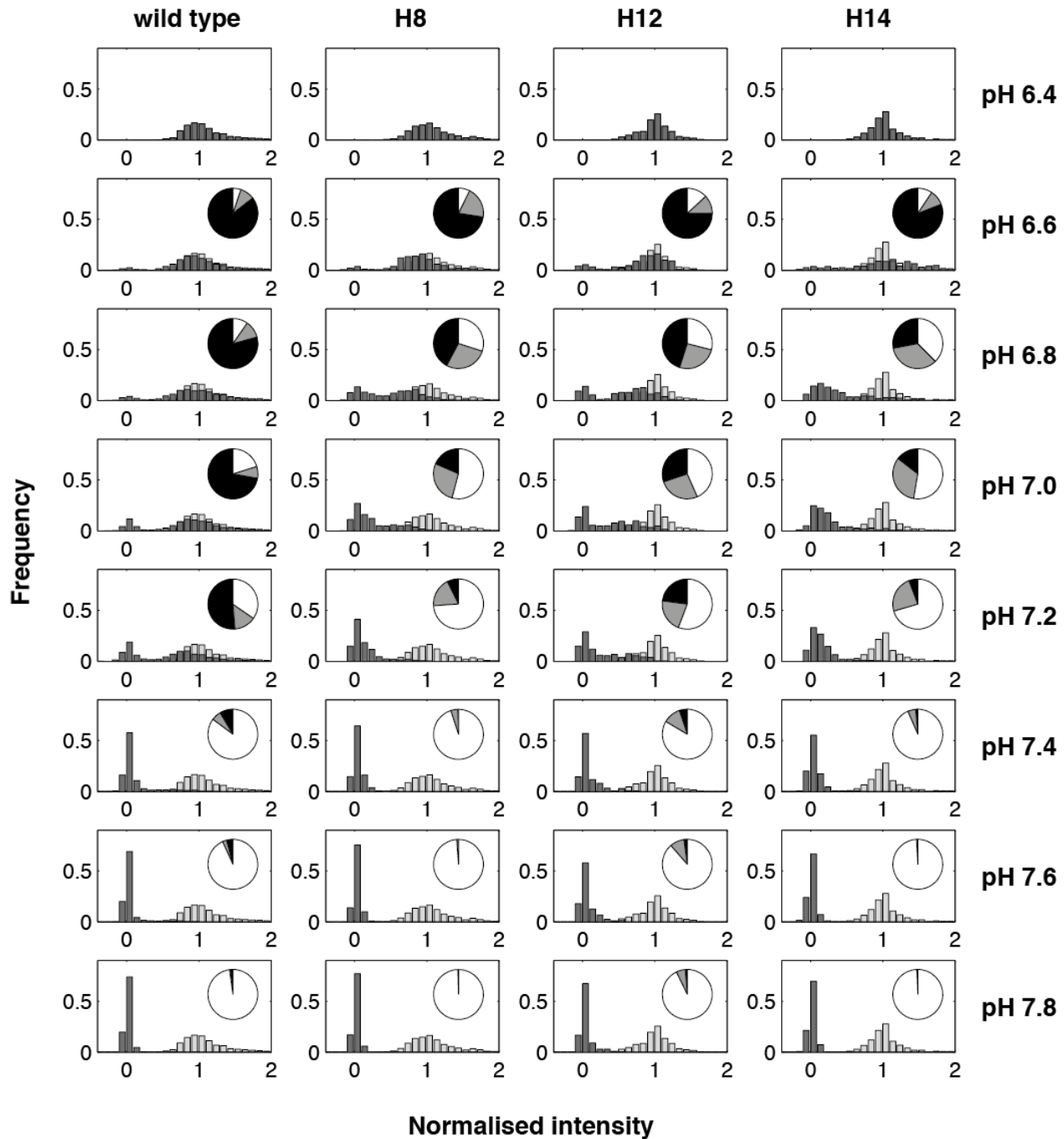

Normalised intensity

Figure S1 (related to Figure 3). pH dependence of coat stability. Histograms of normalized fluorescence intensities of clathrin coats assembled with either wild type or mutant (H8, H12 or H14) clathrin heavy chain and measured after exposure to buffer at various pH values during the coat stability assay. The histograms contain pooled intensities from three separate experiments for each type of clathrin coat (wt or mutant). The intensities were determined on flattened images to correct for the gradient in laser intensity across the field of view. The dark gray histograms represent the distributions measured at the respective pH value. The light gray histograms represent the starting distribution at pH 6.4 and are included for comparison. The fluorescence intensities of intact coats (pH 6.4) follow a broad normal distribution centered at 1. The fluorescence intensities measured at the locations of disassembled coats appear as a narrow distribution close to 0. Partial coats are apparent as signals with an intermediate fluorescence intensity. The pie charts show the fraction of intact coats (black), partial coats (grey) and disassembled coats (white).
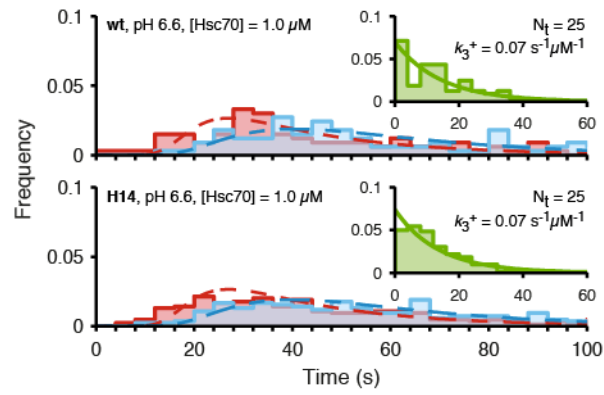
Figure S2 (related to Figure 5). Wild type and H14 mutant clathrin coats uncoat with similar kinetics at pH 6.6. Distributions of Hsc70 accumulation times (red), disassembly times (green) and the times of the entire uncoating reaction (blue) overlaid with fits of the kinetic model. The uncoating reaction was carried out with wild type or H14 mutant coats at pH 6.6 in the presence of 1.0 μM Hsc70.